

Researches on Essential Mechanics Issues for Submerged Floating Tunnel

Y. Hong*, F. Ge & X. Long

State Key Laboratory of Nonlinear Mechanics, Institute of Mechanics, Chinese Academy of Sciences, Beijing, China

*Correspondent: hongys@imech.ac.cn

ABSTRACT: Since 2001, a research group in the Institute of Mechanics, Chinese Academy of Sciences, has been devoted to the research of essential mechanics issues for submerged floating tunnel (SFT). In addition to the structural design of the SFT prototype in Qiandao Lake, the relevant researches cover a number of topics. This paper briefly describes the research procedure and results, including dynamic response of SFT due to surface wave, vortex-induced vibration of anchoring system, structural analysis of curved SFT, temperature effects of curved SFT, structural dynamic response due to accidental load, and effects of structural parameters (buoyancy-weight ratio, tunnel length, tether stiffness, etc.) on dynamic response.

1 INTRODUCTION

Submerged floating tunnel (SFT) i.e. Archimedes Bridge, is a kind of structural passage floating and submerged within water to bridge the banks, which takes the advantage of buoyancy and is tethered to the foundation and the shores. SFT is an innovative transportation technology for the crossing of sea strait, lake or other water sound. It also can be designed and constructed for other applications such as water (oil or gas) supply tube and sightseeing tunnel. As a promising technique, it will become attractive competing with traditional techniques with its economical and environmental advantages (Ahrens 1997).

At present, there is still not an actual SFT being built in the world. To build such a tunnel will encounter various technical problems, such as the architecture design of the tunnel, the configuration of cable systems, the connection design between SFT and shores, the implementation solution of SFT, etc. These difficulties connote mechanics concepts and related mechanics problems are key issues for in depth study (Huang et al. 2002).

Since 1980s, there have been research reports in the aspects of conceptual design and dynamic response by investigators from Italy, Norway, Japan, USA, etc. (Dong et al. 2007a). In China, several research groups from universities and research institutions have involved in SFT researches since late 1990. A research group in the Institute of Mechanics, Chinese Academy of Sciences has been devoted to the research of essential mechanics issues

for SFT since 2001, which covers a number of topics. This paper briefly presents such research progresses, including dynamic response of SFT due to surface wave, vortex-induced vibration of anchoring system, structure analysis of curved SFT, temperature effects of curved SFT, structural dynamic response due to accidental load, and effects of structural parameters on dynamic response. Our other results, e.g. design solutions of SFT prototype, dynamic response due to seismic load, fluid-solid-soil coupling behaviour of foundation and cable system, etc. (Chinese Team of SIJLAB 2007, Yang et al. 2008, 2009, Xiao & Huang 2007) are excluded in this paper.

2 DYNAMIC RESPONSE DUE TO SURFACE WAVE (Chinese Team of SIJLAB 2007)

2.1 Calculation of wave force

For calculating the wave force acting on the SFT, it is necessary to choose appropriate wave theory. The valid method for such a calculation is relied on the ratio of diameter of tunnel D to wave length λ . When D/λ is smaller than 0.2, it is assumed that the presence of SFT is with little influence the propagation of surface wave and the Morison formulation of Eq.(1) can be used to calculate the wave force.

$$F = \frac{1}{2} C_D \rho D (\dot{u}_w + \dot{u}_c - \dot{u}_s) |\dot{u}_w + \dot{u}_c - \dot{u}_s| + \frac{\pi \rho D^2}{4} (C_M \ddot{u}_w - C_a \ddot{u}_s) \quad (1)$$

where, C_D is damping coefficient, C_M is inertial coefficient and C_a is added mass coefficient respectively, with their values relevant to Reynolds

number of the fluid. Also in Eq.(1) \dot{u}_w is the wave induced velocity of water particle, \dot{u}_c is current velocity, \dot{u}_s is structural vibrating velocity, and \ddot{u}_w and \ddot{u}_s are the corresponding accelerations of water particle and structure.

If D/λ is larger than 0.2, however, the presence of SFT will influence the surface wave which means that the Morison formulation is invalid. It is appropriate to use diffraction theory to calculate wave force. The fluid is assumed to be incompressible, inviscid and irrotational. The fluid velocity is then represented at time t by the gradient of the velocity potential $\phi(\mathbf{x}, t)$ satisfying the Laplace equation and the given boundary conditions. Such that

$$\nabla^2 \phi = 0 \quad \text{within fluid} \quad (2)$$

$$-\frac{\omega^2}{g} \phi + \frac{\partial \phi}{\partial z} = 0 \quad \text{at free surface, } z = 0 \quad (3)$$

$$\frac{\partial \phi}{\partial z} = 0 \quad \text{at sea floor, } z = -d \quad (4)$$

$$\frac{\partial \phi}{\partial \mathbf{n}} = 0 \quad \text{on wetted structural surface } S \quad (5)$$

where ω is wave frequency, \mathbf{n} is the wetted surface normal vector. Furthermore, in order to insure that the velocity potential has the correct behavior in the remote field, the Sommerfeld radiation condition is imposed. Once the potential is determined, the total pressure can be obtained from Bernoulli equation and the wave force is calculated by pressure work integration over the wetted structural surface.

2.2 Structural model

Finite element (FE) model is used to approximate SFT structures. The tunnel tube is modeled by beam element based on that the tunnel length is much larger than its characteristic dimension of cross-section. Tether can only be tensioned, not for compression, so it is modeled by truss element. Note that SFT is consisted of a number of tube segments with the same specifications, which are connected together by joints. The joint rigidity has the direct effect on the dynamic response of SFT. According to the rigidity, the joints are classified into two categories. One is rigid joint, the other is semi-rigid joint (or flexible joint). In the FE model, they are modeled by BEAM and SLOT connection elements respectively.

For comparison, two FE models with different types of joint are investigated. For rigid joint model, relative motion between two adjacent segments is restricted. For semi-rigid joint model, relative displacement along the tunnel axis is allowable and

the relative displacements in the other two directions are restricted. Meanwhile rotational degrees of freedom are also available. Table 1 lists the structure parameters for the case study.

Table 1. Characteristic values for SFT

Tunnel length	117 m
Tunnel diameter	4.39 m
Bending stiffness	$2.985 \times 10^{11} \text{ N}\cdot\text{m}^2$
Tether diameter	0.06 m
Young's modulus of tether	$1.4 \times 10^{11} \text{ N/m}^2$
Joint rigidity(for semi-rigid joint)	$1.215 \times 10^6 \text{ N/m}$

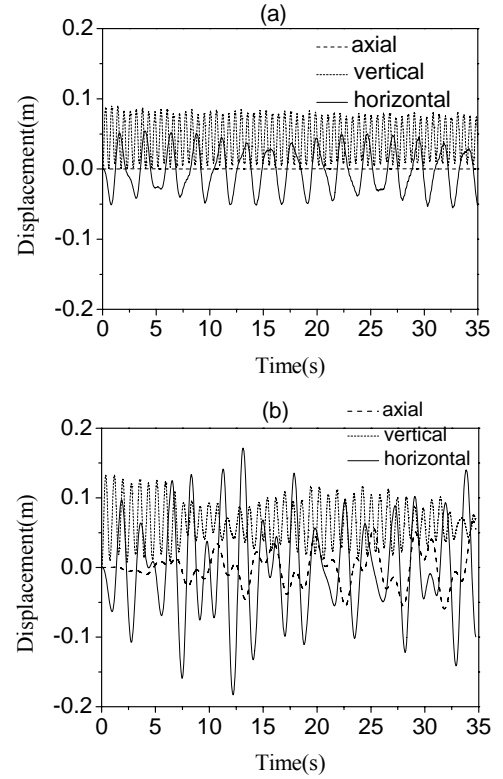


Figure 1. Displacements of tunnel mid-span versus time: (a) rigid joint model, (b) semi-rigid joint model.

In addition, wave height is 1m, wave period is 2.3 sec and wave length is 8.25m. Because of $D/\lambda = 0.532$, diffraction theory is adopted in the calculation. Fig. 1 presents the displacements obtained at the mid-span of tunnel versus time. It is seen that the use of semi-rigid joint decreases the total rigidity of tunnel. Therefore, the amplitudes of tunnel oscillations increase. However, from the stand point of safety, the decrease of total rigidity is beneficial for reducing stress concentration.

Other useful information including relative displacement for semi-rigid joint, distribution of bending moment, shear force in joint, etc. can also be provided based on the presented model.

3 DYNAMIC ANALYSIS OF ACCIDENTAL IMPACT LOAD (Hui et al. 2008)

SFT is located under the water surface. There is a potential risk of collision due to sink ship or other

objects. Therefore, for the safety of SFT, it is important to analyze the structural resistance to impact load.

3.1 Analytical solution

For simplicity, SFT is assumed to be a cylindrical shell with its two ends pinned. The effect of impact object is approximated by concentrated force. The distribution mass of shell is converted to concentrated mass at the impact point.

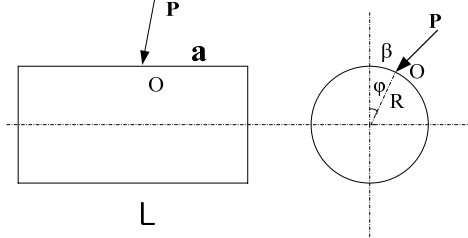


Figure 2. Model of SFT under impact.

By introducing an equivalent mass coefficient e , the shell with distributed mass, as shown in Fig. 2, has been transferred to an elastic system with concentrated mass eM using equivalent mass method. The energy conservative equation during the deformation process is

$$\frac{V^2}{2}[m+e(M+M')] + mg(w_{dy} \cos \varphi + v_{dy} \sin \varphi) = \frac{1}{2}(P_u u_{dy} + P_v v_{dy} + P_w w_{dy}) + W_f \quad (6)$$

where, P_u, P_v, P_w are maximum elastic forces along the three directions at the impact point, u_{dy}, v_{dy}, w_{dy} are corresponding maximum displacements and W_f is the work done by damping force. Relation coefficients of displacement K_1, K_2 ($u_{dy} = K_1 w_{dy}, v_{dy} = K_2 w_{dy}$) and relation coefficients of internal force L_1, L_2 ($P_u = L_1 P_w, P_v = L_2 P_w$) are defined to simplified Eq.(6). Based on the assumption of elastic deformation, the formula $P_w/Q_w = w_{dy}/w_{st}$ is obtained, where Q_w is the weight of impact object and w_{st} is the maximum radial displacement under the object weight. Substituting into Eq.(6), one has

$$\frac{V^2}{2}[m+e(M+M')] + mgw_{dy}(\cos \varphi + K_2 \sin \varphi) = \frac{Q_w w_{dy}^2}{2w_{st}}(1+K_1 L_1 + K_2 L_2) + W_f \quad (7)$$

Eq.(7) is a quadratic equation about w_{dy} which contains 9 unknown variables.

The equivalent mass coefficient is defined as

$$\frac{1}{2} \bar{\rho} h R^2 \int_0^{L/R} \int_0^{2\pi} (\dot{u}^2 + \dot{v}^2 + \dot{w}^2) d\xi d\varphi = \frac{1}{2} eM(\dot{u}^2 + \dot{v}^2 + \dot{w}^2)_p \quad (8)$$

The velocity V after impact is derived using momentum conservation theorem. The added mass

per unit length for cylindrical shell has the form of $m' = C_M \pi \rho_w R^2$, where ρ_w is the fluid density and C_M is the added mass coefficient with the value of 1.0. Fluid damping force is calculated with Morison equation. The integration along displacement path is the work W_f . For the present case, the displacement function is defined as

$$F(\xi, \varphi, t) = C_{mn} \cos(n\varphi) \sin(\lambda_m \xi) \exp(i\omega_{mn} t) \quad (9)$$

where $\lambda_m = m\pi R/L$, ω_{mn} is the natural frequency of shell and ξ is the nondimensional coordinate. Thus, the transient displacements are expressed as

$$\begin{cases} u = -F_{\xi\varphi\varphi} + \mu F_{\xi\xi\xi\xi} \\ v = (2 + \mu)F_{\xi\xi\varphi} + F_{\varphi\varphi\varphi} \\ w = \nabla^4 F = F_{\xi\xi\xi\xi}^{(4)} + 2F_{\xi\xi\varphi\varphi}^{(4)} + F_{\varphi\varphi}^{(4)} \end{cases} \quad (10)$$

Substituting Eq.(9) into (10), one can get the expressions of the relation coefficients of displacement K_1, K_2 . Relation coefficients of internal force L_1, L_2 are derived based on force equilibrium equation of the shell, geometrical relationship and constitutive equations.

If the static loads acting on the shell are known, the radial displacement w_{st} is available by using Galerkin's method based on the dynamic equation of shell with boundary conditions. Last, once the 9 unknown variables are determined, the displacement w_{dy} due to the impact can be obtained by Eq.(7).

3.2 Numerical simulation

Numerical simulation based on the commercial code ANSYS/LS_DYNA is used to demonstrate the analytical solution. In the simulation, the length of tunnel tube is 20m, diameter is 4m and the thickness of wall is 0.1 meter. Shell63 element is used to simulate the tube in the FE model. The Young's modulus of shell material is 2.1×10^5 MPa, density is 7800 kg/m^3 and the Poisson's ratio is 0.3. The impact object is assumed to be rigid and simulated by Solid164 element. The object mass is set as 10 tons and the impact velocity is 3m/s.

Fig. 3 presents the comparison of analytical solution with numerical results for the maximum radial displacement. It is seen that the analytical and numerical results have the same changing tendency with the impact position ξ , the maximum error is less than 25%.

The effects of fluid added mass on the radial displacement and von Mises stress are also shown in Figs. 3 and 4. If the fluid added mass is considered, the radial displacement decreases and the Mises stress increases. The influence of impact velocity is

also investigated. The results show that the radial displacement and Mises stress vary linearly as it increases. If the material of shell is steel Q420 with yield stress of 325MPa, when the impact velocity approaches 4.0m/s, the shell will yield at the impact position (thickness of 0.1m).

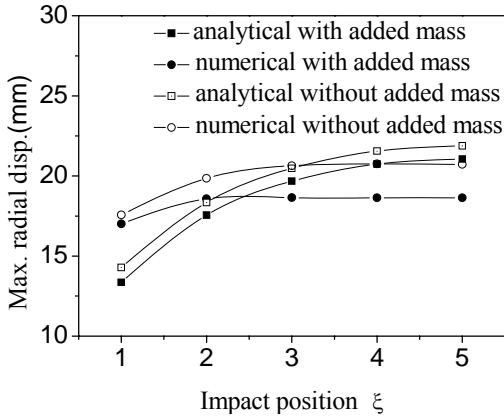


Figure 3. Comparison of impact displacement.

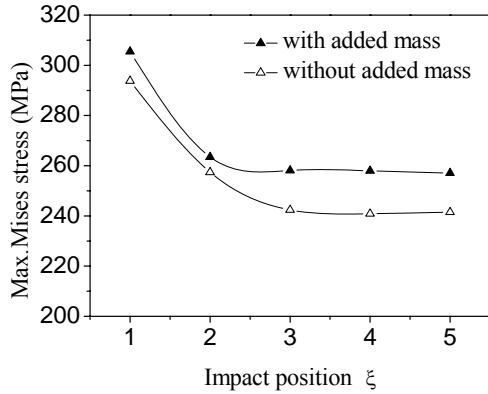


Figure 4. Comparison of impact stress.

4 STRUCTURAL ANALYSIS OF CURVED SFT AND TEMPERATURE EFFECT (Dong et al. 2006)

Due to terrain and environment conditions, a curved type of transition and connection between SFT and banks sometimes needs to be considered so as to decrease the length of tunnel or relax the slope of tunnel. Compared with the straight tunnel, the bending moment of curved SFT is remarkably different. Because that the bending is coupled with the torsion, the torque of curved SFT is of the same order of magnitude as bending moment, while for straight SFT it is much smaller than bending moment and is neglected.

Temperature induced internal force is the concerning problem in the structural analysis of curved SFT. A segment of SFT is considered, with one end connected rigidly with bank and the other end connected elastically with bank. Fig. 5 shows the schematic diagram of the tube. Two pairs of tethers are set to constrain the deformation of tube along the radial direction. The stiffness of tether is

assumed to be k , and the incline angle between the tether and the vertical direction is θ . The radial stiffness is $k_R = k \sin \theta$ and the tangent stiffness is neglected compared to it. When the temperature increases in ΔT , radial displacement at point B due to free deformation is Δ_{BR} . Similarly, Δ_{CR} is denoted at point C. The deformation is elastic. Therefore, the radial force P_{BR} or P_{CR} in tether is obtained with corresponding radial stiffness.

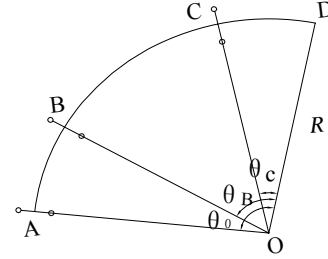


Figure 5. Schematic diagram showing AD being curved tube.

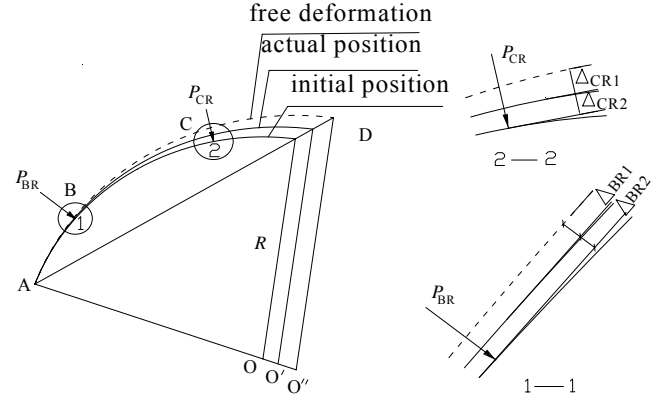


Figure 6. Temperature induced deformation of tube.

As shown in Fig. 6, actual radial displacement Δ_{BR2} , Δ_{CR2} , displacement due to free deformation Δ_{BR} , Δ_{CR} and displacement under the radial force Δ_{BR1} , Δ_{CR1} are satisfying Eq.(11).

$$\begin{cases} \Delta_{BR1} + \Delta_{BR2} = \Delta_{BR} \\ \Delta_{CR1} + \Delta_{CR2} = \Delta_{CR} \end{cases} \quad (11)$$

It is appropriate to assume the SFT to be a quadratic hyperstatic structure in the horizontal plane. The softness factors can be derived using traditional method. Based on the static equilibrium formulation and Eq.(11), Δ_{BR2} and Δ_{CR2} are solved. Moreover, the radial force in tether is obtained under the elastic assumption.

The resultant forces in tether along the vertical direction for one pairs of tethers are consistent but with opposite direction. It means that torsional torque occurred in the cross-section of tube. Due to the coupled of bending and torsion for curved SFT, bending moment along the tube is also created. Therefore, it is important to consider the temperature induced torque for the design of curved SFT.

The stiffness of tether is $9.8 \times 10^7 \text{ N/m}$, bending stiffness of tube is $3.4 \times 10^{10} \text{ N} \cdot \text{m}^2$, incline angle of tether is 30° , $\theta_0 = 0.4, \theta_B = 0.3, \theta_C = 0.1$, radius of curvature of curved SFT equals 100m and the temperature change is 20°C . The effects of some structural parameters on the radial forces in tethers at points B and C are investigated. The numerical results show that the tether stiffness and radius of curvature are two important factors considering the variation of internal force. In the case study, when the tether stiffness is larger than $2.4 \times 10^8 \text{ N/m}$ and radius angle larger than 0.6, the effects of temperature induced internal force need to be considered.

In addition, kinetic formulation of 3-D curved SFT is also derived based on Hamilton principle. (Dong et al. 2007b). These equations indicate that four generalized displacements are coupled with each other. When spatial structure converged into planar curvilinear structure, two generalized displacements in two perpendicular planes are coupled with each other.

5 EFFECTS OF STRUCTURAL PARAMETERS ON DYNAMIC RESPONSE (Long et al. 2009)

The selection and decision of structural parameters is an essential issue in SFT design. Based on the fluid dynamic environment of Qiandao Lake, PR China and the structural designs of the tunnel and cable systems proposed by SIJLAB (Chinese Team of SIJLAB, Italian Team of SIJLAB), the effects of basic structural parameters on dynamic response of SFT under hydrodynamic loads is investigated. The parameters includes structural damp, tunnel length, buoyancy-weight ratio (BWR), cable stiffness coefficients and tunnel net buoyancy.

BWR is a key structural parameter with respect to the SFT structural stability, which is defined as the ratio of tunnel buoyancy to the whole tunnel weight (including weights of tunnel structure, infrastructure, and cable systems). It is undoubted that tunnel buoyancy must be larger than its self-weight and the net buoyancy (the difference between buoyancy and self-weight) is balanced by the cable systems which are connected between tunnel and foundations. Consequently, BWR determines the tension force in the cable section and influences the dynamic behavior of SFT structure, especially the stability of SFT. Furthermore, under service condition, the actual BWR value of SFT is affected by traffic load and crowd load.

After the analysis involving structural damp, the responses of the mid-span of SFTs as a function of BWR in both current direction and vertical direction are shown in Fig. 7, where STDEV is the amplitude

of dynamic responses. As for the dynamic response in the current direction, the value of STDEV increases with the increasing value of BWR. In Fig. 7(b), it is seen that when BWR is 1.2, there is a remarkable trend change in the vertical dynamic response of SFT. Experimental results have also shown the similar trend as the presented numerical results, which demonstrate the effect of BWR on dynamic response of SFT.

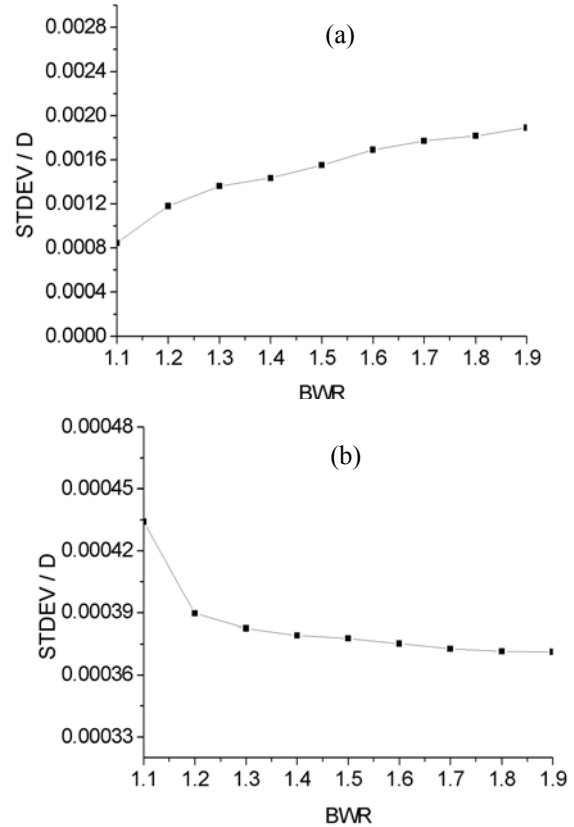


Figure 7. STDEV at SFT mid-span versus BWR: (a) Current direction, (b) Vertical direction.

Other parameters such as tunnel length, tether stiffness etc. are also investigated for the proposed design. The net buoyancy of tunnel segment and the stiffness coefficient of cable systems are significant structural parameters making influence on SFT dynamic responses. Structural damp is an inevitable factor in the analysis of SFT dynamic responses especially in the vertical direction. The effect of SFT tunnel length on dynamic responses can be neglected in the practical design.

6 VORTEX INDUCED VIBRATIONS OF TETHER (Ge et al. 2007a)

When current flows past the tether, vortex is formed along the tether in downstream direction. Force due to vortex shedding is exerted on the tether which causes the tether vibrating. Vortex-induced vibration (VIV) of tether has the potential to cause fatigue failure and it is need to be investigated before to design a real SFT.

One method is used to study VIV is computational fluid dynamics. This procedure is extremely computationally demanding and is hard to be used for engineers. The alternative approach is to model the principle features of vortex shedding using a dynamical system with some semi-experienced parameters. With this approach, Iwan et al. (1981) proposed a analytical procedure for predicting the amplitude of vibration due to vortex shedding. Based on it, the engineering analysis program of vortex-induced transverse vibration of SFT tether is formed. The effect of BWR on VIV of tether is investigated.

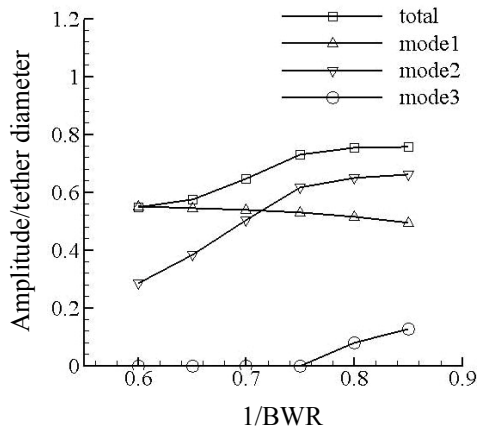


Figure 8. Amplitude of tether VIV versus BWR.

In the case study, the length of tether equals 252m, its diameter is 1.1176m and the wall thickness is 0.038m. The flow is of shear current feature. Fig. 8 shows how the amplitude of tether VIV varies with BWR. Due to the shear current effect, more vibration modes are excited as BWR decreases and the total amplitude of tether increases too. The results mean that BWR is definitely a key parameter for tether VIV, as it determines the value of tension force in tether therefore the natural frequency of tether is also influenced by BWR.

Some other aspects concerning with tether VIV are also discussed (Ge et al. 2006, 2007b, 2009). We put focus on the coupling effect between in-line and cross-flow vibrations. Wake oscillator model is adopted to simulate the vortex dynamics. The numerical results obtained by the proposed model are testified with some experimental data. The comparison shows good agreement has been reached and the proposed model can be used to simulate 2-D vibrations of tether.

7 CONCLUDING REMARKS

The research progresses on essential mechanics issues for SFT obtained by our team have been summarized. The topics cover dynamic response of SFT due to surface wave, VIV of tether, structure analysis of curved SFT, temperature effects of

curved SFT, dynamic response due to accidental load and effects of structural parameters on dynamic response.

ACKNOWLEDGMENTS

This work is supported by National Natural Science Foundation of China (no. 10532070) and Knowledge Innovation Program of Chinese Academy of Sciences (no. KJCX2-YW-L07).

REFERENCES

- Ahrens, D. (1997) *Submerged Floating Tunnels--- A Concept Whose Time Has Arrived*. *Tunneling and Underground Space Technology*, 12: 317-336.
- Chinese Team of SIJLAB (2007) *Report of research and design for Archimedes Bridge Prototype at Qiandao Lake*. Institute of Mechanics, Chinese Academy of Sciences.
- Dong, M., Ge, F., Hong, Y. (2006) *Analysis of thermal internal forces for curved submerged floating tunnel*. *Eng Mech*, 23(sup.I): 21-24. (In Chinese)
- Dong, M., Ge, F., Hui, L., Hong Y. (2007a) *Research progress in submerged floating tunnels*. *China Journal of Highway and Transport*, 20: 101-107. (In Chinese).
- Dong, M., Ge, F., Zhang, S., Hong, Y. (2007b) *Dynamic equations for curved submerged floating tunnel*. *Appl Math Mech*, 28: 1299-1308.
- Ge, F., Dong, M., Hui, L., Hong, Y. (2006) *Vortex-induced vibration of submerged floating tunnel tethers under wave and current effects*. *Eng Mech*, 23(sup.I): 217-221. (In Chinese)
- Ge, F., Hui, L., Hong, Y. (2007a) *Vortex-induced vibration of submerged floating tunnel tethers in shear current*. *Journal of the Graduate School of CAS*, 24:351-356. (In Chinese).
- Ge, F., Hui, L., Hong, Y. (2007b) *Vortex induced nonlinear vibrations of submerged floating tunnel tethers*. *China J Highway Transport*, 20: 85-89. (In Chinese).
- Ge, F., Long, X., Wang, L., Hong, Y. (2009) *Flow-induced vibrations of long cylinders modeled by coupled non-linear oscillators*. *Science in China Series G: Physics, Mechanics & Astronomy*. In press.
- Huang, G., Wu, Y., Hong Y. (2002) *Transportation of Crossing Waterways via Archimedes Bridge*. *Ship Building of China*, 43 (sup.): 13-18. (In Chinese)
- Hui, L., Ge, F., Hong, Y. (2008) *Calculation model and numerical simulation of submerged floating tunnel subjected to impact loading*. *Eng Mech*, 25: 209-213. (In Chinese).
- Italian Team of SIJLAB (2007) *Design Report of the Archimede's Bridge Prototype in Qiandao Lake (P.R of China)*. Italy.
- Long, X., Ge, F., Wang, L., Hong, Y. (2009a) *Effects of fundamental structure parameters on dynamic responses of submerged floating tunnel under hydrodynamic loads*. *Acta Mech Sinica*, DOI:10.1007/s10409-009-0233-y.
- Xiao, J., Huang, G. (2007) *Effects of tunnel-shore connection mode on seismic response of SFT*. *Proc 16th National Conf on Struct Eng*, No. 1: 501-504. (In Chinese).
- Yang B., Gao F., Wu Y. (2008) *Flow-induced vibrations of a cylinder with two degrees of freedom near rigid plane boundary*. *Int J Offshore Polar Eng*, 18: 302-307.
- Yang, B., Gao, F., Jeng, D., Wu, Y. (2009): *Experimental study of vortex-induced vibrations of a cylinder near a rigid plane boundary in steady flow*, *Acta Mech Sinica*, 25: 51-63.